

# Statistical properties of inelastic Lorentz gas

Kim Hyeon-Deuk and Hisao Hayakawa

*Graduate School of Human and Environmental Studies, Kyoto University, Sakyo-ku, Kyoto  
606-8501, Japan*

## Abstract

The inelastic Lorentz gas in cooling states is studied. It is found that the inelastic Lorentz gas is localized and that the mean square displacement of the inelastic Lorentz gas obeys a power of a logarithmic function of time. It is also found that the scaled position distribution of the inelastic Lorentz gas has an exponential tail, while the distribution is close to the Gaussian near the peak. Using a random walk model, we derive an analytical expression of the mean square displacement as a function of time and the restitution coefficient, which well agrees with the data of our simulation. The exponential tail of the scaled position distribution function is also obtained by the method of steepest descent.

PACS numbers: 66., 05.40.Fb, 05.60.Cd, 74.80.Bj

arXiv:cond-mat/0012325v1 [cond-mat.stat-mech] 18 Dec 2000

## I. INTRODUCTION

A system of inelastic hard disks is important as the simplest model for a collection of inelastic particles. It is believed that the inelastic Boltzmann gas model is a realistic model of granular gases which are typical examples of collections of inelastic particles. [1–3] Several investigations have been carried out on the scaled velocity distribution function of the inelastic gas for the inelastic Boltzmann equation, where the approximate analytical solution of the inelastic Boltzmann equation has been obtained. [3–9] They also suggested that the scaled velocity distribution function of the inelastic Boltzmann equation has an exponential high energy tail, which was confirmed in simulations of smooth hard inelastic disks in the homogeneous cooling state. [3,5,6]

There is, however, the strong restriction in the applicability of the inelastic Boltzmann equation. Inelastic collisions generate clusters of the inelastic disks in a cooling state. Thus, the inelastic Boltzmann equation which is only valid for dilute cases becomes no longer valid as time goes on.

On the other hand, the inelastic scatterings of classical electrons by ions can be modeled by the inelastic Lorentz gas in which few fraction of particles can move freely among many immobile scatters. [10] Since the fixed scatters keep their initial configuration, the system can keep the dilute state if the initial configuration is dilute. We also indicate that there are many examples of the inelastic Lorentz gas in the natural phenomena such as the solid metal, the solid electrolyte and the spontaneous interparticle percolation. [10] The Lorentz gas is also familiar in dairy life such as the pedestrian motion among a cloud of persons and obstacles, the pachinko game and the pinball game etc. There is an additional advantage that the analysis of the inelastic Lorentz gas is easier than that of the inelastic Boltzmann equation because the inelastic Lorentz gas model is the one-body problem. Wilkinson and Edwards [10] have analyzed the steady velocity distribution function of inelastic Lorentz gas under the uniform external field. We believe, however, that we need systematic studies of the inelastic Lorentz gas in simpler situations. In particular it is important to discuss the

spatial structure of the inelastic Lorentz gas without any external field as the first step of the study of this system. Thus, we intend to investigate the statistical properties of the inelastic Lorentz gas including its spatial structure in the cooling state in this paper.

The organization of this paper is as follows. In section II, we introduce the model of our simulation. In section III, we validate our simulation code by evaluating the mean square displacement, the velocity distribution and the position distribution in elastic collisions. We also explain the main results of our simulation and analysis for the mean square displacement and the position distribution of the inelastic Lorentz gas. We conclude our results in section IV.

## II. THE MODEL OF OUR SIMULATION

In our simulation we adopt the event driven method for hard core collision of particles. [11] The system consists of 40000 fixed smooth hard disks, that is 40000 scatters, and one tracer disk. The collision between the tracer and the scatters is inelastic hard core collision with a constant coefficient of restitution  $e$ . Through our simulation, we use dimensionless quantities in which the scales of length and velocity are respectively measured by the diameter of the disks  $d$  and the variance of the initial velocity distribution  $U$ . Namely, both of all the scatters and the tracer are circular disks with their diameter  $d$ . The number density of the scatters in this system is  $0.04d^{-2}$ , where the system size is  $L_x = L_y = 1000d$ . The area fraction is approximately 0.0314. We adopt the periodic boundary condition in this system. The system size is enough large to remove the boundary effect of this system, because the tracer is localized and have rarely gone across the boundaries. We average each result over 10000 samples which consist of 100 different initial configurations of the scatters and 100 different initial velocities of the tracer. Each initial configuration of the scatters is at random. Each tracer starts from the center of the system and its distribution of the initial velocities is made from normal random numbers, where its average is zero and its variance is  $U$ . Each sample has been calculated until 100 inelastic collisions. In each inelastic collision,

the velocity of a tracer tangential to the collision plane are preserved, while the velocity normal to it changes with the restitution coefficient  $e$  which is assumed to be a constant for all the collisions. The precollision velocity of the tracer  $\mathbf{v}^*$  yields the postcollision velocity of it  $\mathbf{v}$  with  $\mathbf{v} \cdot \hat{\sigma} = -e(\mathbf{v}^* \cdot \hat{\sigma})$ , where  $\hat{\sigma}$  is a unit vector pointing from the center of the scatter to the center of the tracer ( Fig.1 ). Thus, the expression is given by

$$\mathbf{v} = \mathbf{v}^* - (1 + e)(\mathbf{v}^* \cdot \hat{\sigma})\hat{\sigma}. \quad (1)$$

In the simulation of the inelastic Lorentz gas, the velocity of the tracer quickly decreases. For the sake of long time simulation, we adopt the rescaling of the speed of the tracer as follows. After each collision, the magnitude of the postcollision velocity  $|\mathbf{v}|$  has been put to that of the precollision velocity  $|\mathbf{v}^*|$ , i.e. the magnitude of the initial velocity of the tracer has been preserved for all the collisions in each sample. Note that we use non-scaled values of  $\mathbf{v}$  for our analysis.

### III. RESULTS:SIMULATION AND THEORY

Now, we explain the main results of our simulation and analysis for inelastic Lorentz gas. We study the mean square displacement and the position distribution of the tracer.

#### A. Check of our simulation code

Our simulation code has been validated by the test simulation in which we have evaluated the mean square displacement, the velocity distribution and the position distribution of the tracer in the elastic collisions, i.e.  $e = 1$ . For elastic scatters, we expect that the tracer displays random walk motion when the initial speeds of the tracer are identical and that the Gaussian is the stable velocity distribution.

Corresponding to a random walk model, we have fixed the magnitudes of 100 different initial velocities of the tracer, i.e.  $|\mathbf{v}_0| = U$ . In each sample, we calculate the motion of tracer until 10000 elastic collisions. The other conditions of the test simulation are same as those

of the simulation in inelastic collisions. We have checked that the mean square displacement of the tracer  $\langle \mathbf{r}^2(t) \rangle$  is almost a linear function of time, where  $\langle \cdot \cdot \cdot \rangle$  indicates the average over the 10000 samples. We also confirm that all the data of the position distribution  $g(r, t)$  can be scaled as

$$g(r, t) = \frac{1}{\sqrt{\langle \mathbf{r}^2(t) \rangle}} G(R), \quad (2)$$

where  $G(R)$  is the scaled position distribution function and  $R \equiv r/\sqrt{\langle \mathbf{r}^2(t) \rangle}$  is the scaled distance from the center of the system at which the tracer started. We check that the scaled position distribution  $G(R)$  is almost on the Gaussian curve as expected from the conventional random walk. Furthermore, the velocity distribution of the tracer becomes almost the Gaussian.

### B. The mean square displacement

Let us discuss the statistical properties of inelastic Lorentz gas. At first, we evaluate the time evolution of the thermal velocity and discuss the mean square displacement in the inelastic system.

In the inelastic Lorentz gas system, many inelastic collisions happen at random. The average number of collision times per unit time is evaluated as  $2dv_0(t)\rho_0$ , where  $d$  is the diameter of the tracer and the scatters and  $\rho_0$  is the number density of the scatters. The thermal velocity  $v_0(t)$  is defined as

$$v_0(t) \equiv \sqrt{\frac{1}{n} \int \mathbf{v}^2 f(\mathbf{v}, t) d\mathbf{v}}, \quad (3)$$

with the velocity distribution of the tracer  $f(\mathbf{v}, t)$  and the average density of the tracer  $n \equiv \int f(\mathbf{v}, t) d\mathbf{v}$ . Therefore the temperature of the system is denoted as

$$T(t) = \frac{1}{2} m v_0^2(t), \quad (4)$$

where  $m$  is the mass of the tracer. [3,7]

In each collision, the energy loss of the tracer is considered to be proportional to the temperature of the system  $T(t)$ . Thus, we can estimate the energy loss of the tracer per unit time as

$$\frac{dT(t)}{dt} = -2dv_0(t)\rho_0h(e)T(t), \quad (5)$$

where  $h(e)$  is a dimensionless function of the restitution coefficient  $e$ . Substitution of eq. (4) into eq. (5) leads to

$$\frac{dv_0(t)}{dt} = -d\rho_0h(e)v_0^2(t). \quad (6)$$

Solving eq. (6), we obtain the thermal velocity  $v_0(t)$  as

$$v_0(t) = \frac{1}{\frac{1}{v_0(0)} + d\rho_0h(e)t}, \quad (7)$$

where  $v_0(0)$  is the initial thermal velocity.

Here, we can deduce the expression of  $h(e)$  from our simulation as follows. Figure 2 shows  $(v_0^{-1}(t) - v_0^{-1}(0))/(1 - e)U$  versus  $tUd^{-1}$  plots for several values of the restitution coefficient, namely, for  $e = 0.4, 0.6, 0.7$  and  $0.9$ . All the data are on the same straight line which is also shown in Fig.2. Corresponding to the results of our simulation, we set the number density of the scatters  $\rho_0 = 0.04d^{-2}$  and the initial thermal velocity  $v_0(0) = \langle v_0(0) \rangle_0 = \sqrt{\pi/2}U$ , where  $U$  is the variance of the initial velocity distribution and  $\langle \cdot \cdot \rangle_0$  denotes an average over the initial velocity distribution function  $f_0(v_0(0)) = (2\pi U^2)^{-1} \exp(-v_0(0)^2/(2U^2))$ . Thus, Fig.2 indicates that  $h(e)$  is a linear function of the restitution coefficient  $e$  as

$$h(e) \simeq 1.45 \times (1 - e). \quad (8)$$

To simplify the expressions, let us introduce  $\alpha$  and  $\beta$  as,

$$\alpha \equiv \frac{1}{v_0(0)}, \quad \beta \equiv d\rho_0h(e). \quad (9)$$

Using  $\alpha$  and  $\beta$ , the average time interval  $\tau_N$  from  $N - 1$ th collision to  $N$ th collision between the tracer and the scatters is given as,

$$\tau_N \simeq \frac{l}{v_0(t_{N-1})} = l(\alpha + \beta t_{N-1}), \quad (10)$$

where  $l$  denotes the mean free path of the tracer, and  $t_{N-1}$  is the total time until the  $N-1$ th collision. From the relation  $t_{N-1} = \tau_1 + \tau_2 + \dots + \tau_{N-1}$ , we obtain  $\tau_N$  as a function of the number of collision times  $N$ ,

$$\tau_N = l\alpha(1 + l\beta)^{N-1}. \quad (11)$$

Therefore the total time until the  $N$ th collision  $t_N$  is given by

$$t_N = \tau_1 + \tau_2 + \dots + \tau_N = \frac{\alpha}{\beta} \{(1 + l\beta)^N - 1\}. \quad (12)$$

Rearranging eq.(12), the number of collision  $N$  is obtained as a function of the total time until the  $N$ th collision  $t_N$  as

$$N = \frac{\ln(\frac{\beta}{\alpha}t_N + 1)}{\ln(1 + l\beta)}. \quad (13)$$

Note that eq.(13) holds even for the elastic limit

$$N \rightarrow \frac{t_N}{\alpha l} \quad \text{for } e \rightarrow 1. \quad (14)$$

Here we have used the result of eq.(8), i.e.  $h(e) \rightarrow 0$  for  $e \rightarrow 1$ .

If we assume that inelastic Lorentz gas system corresponds to the random walk system with the reduction of hopping velocity, the effect of inelasticities can be absorbed in the number of collisions  $N$ . Thus, we deduce the expression of mean square displacement of a tracer as

$$\langle \mathbf{r}^2(t) \rangle_e = l^2 N \simeq l^2 \frac{\ln(\frac{\beta}{\alpha}t + 1)}{\ln(1 + l\beta)}, \quad (15)$$

where we use eq.(13) and the suffix  $e$  of the bracket emphasizes the quantity with the restitution coefficient  $e$ . Now, we evaluate some physical quantities in eq.(15). Using the values of our simulation, we obtain  $\alpha = \sqrt{2/\pi}U^{-1}$ ,  $\beta \simeq 0.058 \times (1 - e)d^{-1}$  from Eqs.(8) and (9). We adopt the *effective* mean free path of the tracer as  $l \simeq 13.5d$  instead of the actual mean free path  $l = 12.5d$ .

Substituting these physical quantity and eq.(8) into eq.(15), we obtain the mean square displacement as a function of time and restitution coefficient. Figure 3 shows  $\langle \mathbf{r}^2(t) \rangle_e \times \ln(1 + l\beta)d^{-2}$  versus  $(1 - e)tUd^{-1}$  plots for  $e = 0.4, 0.6, 0.7$  and  $0.9$ . All the results of our simulation shown as the symbols are on the same curve. Our results clearly demonstrates that the tracer is localized in the case  $e < 1$  and that the mean square displacement seems to obey a power of the logarithmic function of time. It should be emphasized that eq.(15), shown in Fig.3, becomes identical with the results of our simulation as time goes on. The reason why eq.(15) deviates a little from the data of our simulation in the early time region in Fig.3 is that few collisions have happened in this region.

### C. Position distribution

In the inelastic Lorentz gas system, the original position distribution function of the tracer  $g_e(r, t)$  for the restitution coefficient  $e$  is scaled by the mean square displacement  $\langle \mathbf{r}^2(t) \rangle_e$ . The scaled position distribution function of the tracer  $G(R)$  is defined as

$$G(R) \equiv \sqrt{\langle \mathbf{r}^2(t) \rangle_e} \times g_e(r, t), \quad (16)$$

where  $R \equiv r/\sqrt{\langle \mathbf{r}^2(t) \rangle_e}$  is the scaled distance from the center of the system at which the tracer started.  $G(R)$  is independent of the restitution coefficient  $e$  and time. Let us study the scaled position distribution of the tracer  $G(R)$ . Figure 4 shows the results of our simulation and analysis. The symbols are results of our simulation which show the scaled position distribution of the tracer for  $e = 0.4, 0.6, 0.7$  and  $0.9$  at four different times  $t = 3000dU^{-1}, 300dU^{-1}, 500dU^{-1}$  and  $100dU^{-1}$ , respectively. All the data of the scaled position distribution  $G(R)$  are almost on the universal curve. It should be noted that the curve is close to a Gaussian near its peak, while the tail seems to obey an exponential function.

On the other hand, the broken line and the dash-dotted line in Fig.4 are results of our theoretical analysis which will be explained later. The broken line corresponds to the data in the tail region of the scaled position distribution, while the dash-dotted line corresponds

to the data in the peak region of the scaled position distribution. Theoretical curves will explain the result of our simulation. Now, let us explain how to obtain the theoretical curves.

At first, we assume that the tracer obeys a renormalized diffusive motion. Thus, the original velocity-position distribution function of the tracer  $g_e(r, \mathbf{v}, t)$  is expected to be given by

$$g_e(r, \mathbf{v}, t) \equiv \frac{1}{2D_0 t} r e^{-\frac{r^2}{4D_0 t}}. \quad (17)$$

Here we assume the diffusion *coefficient*  $D_0$  obeys

$$D_0 \equiv \mathbf{v}^2 \tau = \mathbf{c}^2 v_0^2(t) \tau = \mathbf{c}^2 v_0(t) l, \quad (18)$$

where  $\tau$  is the average time interval between two adjacent collisions,  $l$  is the mean free path of the tracer, and the scaled velocity  $\mathbf{c}$  is defined as  $\mathbf{c} \equiv \mathbf{v}/v_0(t)$ . From eqs.(18) , (7) and (9) , we obtain

$$4D_0 t \simeq \frac{4\mathbf{c}^2 l}{\beta}, \quad (19)$$

for the late stage. Introducing  $\eta$  as

$$\eta \equiv \frac{2D_0 t}{\mathbf{c}^2 \langle \mathbf{r}^2(t) \rangle_e}, \quad (20)$$

we obtain the expression of  $\eta$  for large  $t$  as

$$\eta \simeq \frac{2l}{\beta \langle \mathbf{r}^2(t) \rangle_e} = \frac{2 \ln(1 + l\beta)}{\beta l \ln(\frac{\beta}{\alpha} t + 1)}, \quad (21)$$

where we use eqs.(19) and (15). Thus, from eqs.(17) and (20), we can derive the scaled velocity-position distribution function of the tracer  $G(R, \mathbf{c})$  as

$$G(R, \mathbf{c}) = \frac{1}{\eta \mathbf{c}^2} R e^{-\frac{R^2}{2\eta \mathbf{c}^2}}. \quad (22)$$

In our simulation, all the data of the scaled velocity distribution of the tracer  $f(\mathbf{c})$  can be fitted by the Maxwell-Boltzmann distribution  $\pi^{-1} e^{-\mathbf{c}^2}$  as Fig.5 shows. Thus, the scaled position distribution function  $G(R)$  is expressed by

$$G(R) = \int_{-\infty}^{\infty} \frac{e^{-c^2}}{\pi} \frac{1}{\eta c^2} R e^{-\frac{R^2}{2\eta c^2}} dc = \frac{2}{\eta} R \int_0^{\infty} e^{-p(c,R)R^2} dc. \quad (23)$$

The second equality in eq.(23) defines  $p(c, R)$  as

$$p(c, R) \equiv \frac{\ln c}{R^2} + \frac{c^2}{R^2} + \frac{1}{2\eta c^2}. \quad (24)$$

We analyze eq.(23) by the method of steepest descent in order to obtain the tail region of the scaled position distribution function. Designating  $c$  which satisfies  $\partial p(c, R)/\partial c = 0$  as  $c^*(R)$ , the expression of  $c^*(R)$  is

$$c^*(R) = \sqrt{-\frac{1}{4} + \frac{\sqrt{\eta + 8R^2}}{4\sqrt{\eta}}}. \quad (25)$$

By the method of steepest descent, from eq.(23) we can derive the approximate  $G(R)$ , i.e.

$$G(R) \simeq \frac{2}{\eta} R \int_0^{\infty} \exp[-p(c^*, R)R^2 - \frac{(c - c^*)^2}{2} \frac{\partial^2 p(c^*, R)}{\partial c^2} R^2] dc = \frac{2}{\eta} \sqrt{\frac{\pi}{2 \frac{\partial^2 p(c^*, R)}{\partial c^2}}} e^{-p(c^*, R)R^2}. \quad (26)$$

Equation (26) is reduced to

$$G(R) \simeq \sqrt{\frac{\pi R}{2\sqrt{2}\eta^{\frac{3}{2}}}} e^{-\sqrt{\frac{2}{\eta}}R}, \quad (27)$$

in the limit of  $R \rightarrow \infty$ . Thus, we have shown that the tail of  $G(R)$  obeys an exponential law. Now we use

$$G(R) = \frac{2\gamma}{\eta} \sqrt{\frac{\pi}{2 \frac{\partial^2 p(c^*, R)}{\partial c^2}}} e^{-p(c^*, R)R^2}, \quad (28)$$

instead of eq.(26). Here  $\gamma$  is a fitting parameter. We estimate  $\eta \simeq 0.25$  and  $\gamma \simeq 7.39$  from the comparison of eq.(28) and the data of our simulation on the scaled position distribution in the tail region.

In order to obtain the peak region of the scaled position distribution function, we replace  $c$  in eq.(22) by constant  $\bar{c}$ . Thus, eq.(23) becomes

$$G(R) \simeq \frac{1}{\eta \bar{c}^2} R e^{-\frac{R^2}{2\eta \bar{c}^2}}. \quad (29)$$

Thus, we expect the Gaussian near the peak. Although  $\eta$  in eq.(29) is different from  $\eta$  in eq.(28) in general, we can also obtain the peak region of the scaled distribution function from eq.(29) with the same  $\eta$  as that of the tail region, i.e.  $\eta \simeq 0.25$  if we adopt the point of inflection of the speed distribution function as  $\bar{c}$ , i.e.  $\bar{c} = \sqrt{3/2}$ .

In Fig.4, eq.(28) with  $\eta = 0.25$  and  $\gamma = 7.39$  is expressed by the broken line, while eq.(29) with the same  $\eta$  and  $\bar{c} = \sqrt{3/2}$  is expressed by the dash-dotted line. Figure 4 shows that eq.(28) is in good agreement with the simulation data of the scaled position distribution in the tail region, while the data of our simulation on the scaled position distribution in the peak region are well-fitted by eq.(29).

#### IV. CONCLUSIONS

We have found that the mean square displacement of the inelastic Lorentz gas obeys a power of the logarithmic function of time and that the scaled position distribution of the inelastic Lorentz gas has an exponential tail, while the peak is the Gaussian. We have analytically derived the mean square displacement as a function of time and restitution coefficient which is identical with the data of our simulation. We also analytically obtained the scaled position distribution function the tail of which is exponential and the peak of which is the Gaussian.

#### V. ACKNOWLEDGMENTS

We thank S. Takesue, Ooshida. T, and K. Ichiki for the useful comments. K. H.-D. appreciates A. Awazu, H. Kuninaka, S. Wada and N. Yajima for various advice. This study is partially supported by Grant-in-Aid for Science Research Fund from the Ministry of Education, Science and Culture (Grant No. 11740228).

## REFERENCES

- [1] C.S. Campbell, *Ann. Rev. numer. Fluid Mech.*, **22**, 57 (1990).
- [2] see e.g. L. P. Kadanoff, *Rev. Mod. Phys.* **71**, 435 (1999); P. G. de Gennes, *ibid*, S374 (1999).
- [3] T.P.C. van Noije and M.H. Ernst, *Granular Matter* **1**, 57 (1998).
- [4] S.E. Esipov and T. Poschel, *J. Stat. Phys.* **86**, 1385 (1997).
- [5] J. J. Brey, M.J. Ruiz-Montero and D.Cubero, *Phys. Rev. E* **54**, 3664 (1996).
- [6] J. J. Brey, D. Cubero and M.J. Ruiz-Montero, *Phys. Rev. E* **59**, 1256 (1999).
- [7] Nikolai V. Brilliantov and Thorsten Pöschel, *Phys. Rev. E* **61**, 2809 (2000).
- [8] Teruhisa S. Komatsu, *J. Phys. Soc. Jpn.* **69**, 5 (2000).
- [9] M. Huthmann, J.A.G. Orza and R. Brito, *cond-mat/0004079* (2000).
- [10] D.R. Wilkinson and S.F. Edwards, *F.R.S., Proc. R. Soc. Lond.* **A381**, 33 (1982).
- [11] see e.g. D.C. Rapaport, *J. Comput. Phys.* **34**, 184 (1980).

FIGURES

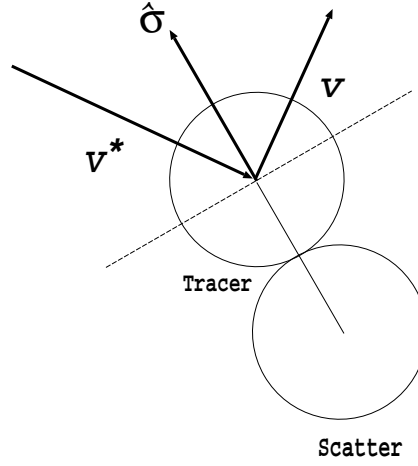


FIG. 1. Unit vector  $\hat{\sigma}$  pointing from the center of a scatterer to the center of a tracer. The precollision velocity of the tracer and the postcollision velocity of it are expressed as  $\mathbf{v}^*$  and  $\mathbf{v}$ , respectively.

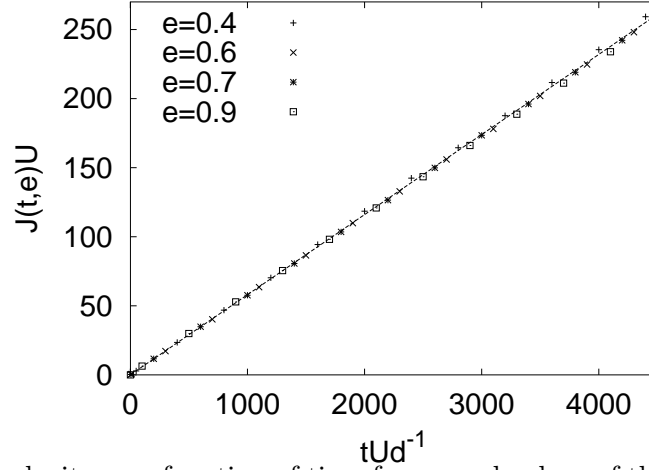


FIG. 2. Thermal velocity as a function of time for several values of the restitution coefficient  $e$ . Note that  $J(t, e) \equiv (v_0^{-1}(t) - v_0^{-1}(0))/(1 - e)$ . The straight line  $0.058 \times tUd^{-1}$  shown as the broken line is the best fitting function of the results of our simulation.

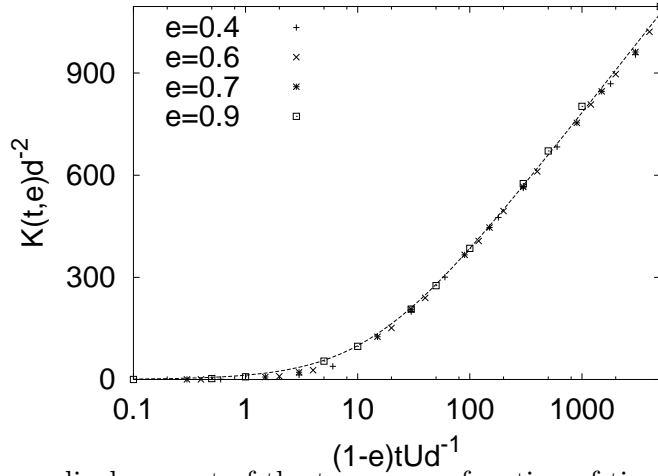


FIG. 3. Mean square displacement of the tracer as a function of time for several values of the restitution coefficient  $e$ . Note that  $K(t, e) \equiv \langle \mathbf{r}^2(t) \rangle_e \times \ln(1 + l\beta)$ . The symbols are results from our simulation. The broken line is obtained from eq.(15) with  $l \simeq 13.5d$  and  $\beta \simeq 0.058 \times (1 - e)d^{-1}$ .

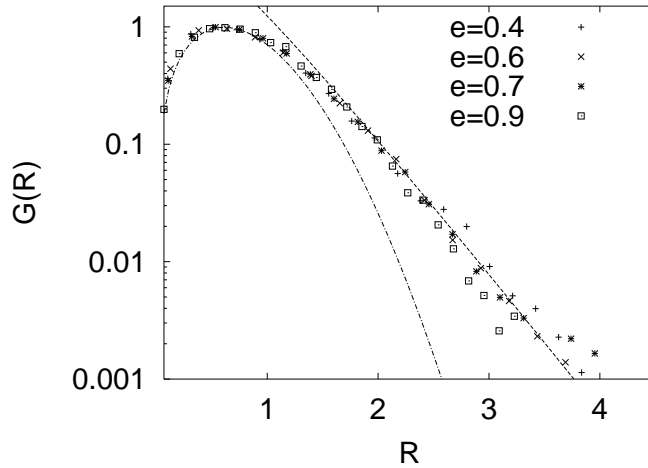


FIG. 4. Scaled position distribution of the tracer  $G(R) = \sqrt{\langle \mathbf{r}^2(t) \rangle_e} \times g_e(r, t)$  as a function of the scaled distance  $R \equiv r / \sqrt{\langle \mathbf{r}^2(t) \rangle_e}$  from the center of the system at which the tracer started. The symbols are the data of our simulation which are plotted for several values of the restitution coefficient  $e = 0.4, 0.6, 0.7$  and  $0.9$  at four different times  $t = 3000dU^{-1}, 300dU^{-1}, 500dU^{-1}$  and  $1000dU^{-1}$ , respectively. The broken line and the dash-dotted line are the approximate solutions of  $G(R)$ . The simulation data in the tail region correspond to eq.(28) with  $\eta = 0.25$  and  $\gamma \simeq 7.39$ , while the simulation data in the peak region correspond to eq.(29) with the same  $\eta$  and  $\bar{c} = \sqrt{3/2}$ .

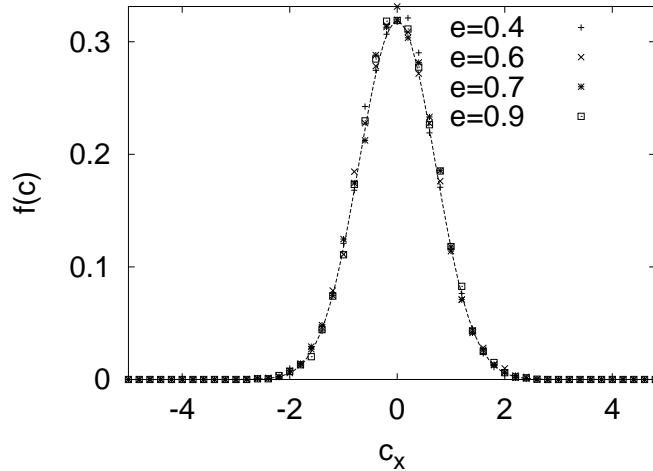


FIG. 5. Scaled velocity distribution of the tracer  $f(\mathbf{c})$  as a function of  $c_x$ . The symbols are data of our simulation. The data are plotted for several values of the restitution coefficient  $e = 0.4, 0.6, 0.7$  and  $0.9$  at four different times  $t = 3000dU^{-1}, 300dU^{-1}, 500dU^{-1}$  and  $1000dU^{-1}$ , respectively. The broken line is the Maxwell-Boltzmann distribution  $\pi^{-1}e^{-\mathbf{c}^2}$ .